Semifluorinated, kinked polyarylenes *via* direct arylation polycondensation†

Fabian Kempe, [a] Felix Riehle,[b] Hartmut Komber,[c] Rukiya Matsidik,[a] Michael Walter [d] and Michael Sommer *[a]

Semifluorinated, amorphous polyarylenes P*mmp*F4 with kinked backbone structure were prepared from a *meta*-substituted, biphenol-based monomer with varying alkoxy substituents R and 1,2,4,5-tetrafluoro-benzene (pF4) *via* direct arylation polymerization (DAP). The chemistry employed is simple, scalable and does not rely on tedious purification techniques. Polycondensation occurs cleanly without major side reactions. Despite the clean polycondensation reaction, very high molar mass materials are difficult to obtain, which is ascribed to an unusual solubility behavior compared to non-fluorinated analogs, and similar, yet more linear tetrafluorobenzene copolymers based on fluorene or carbazole. In order to investigate this phenomenon further, the side chain-dependent properties P*mmp*F4 are investigated using linear, branched and cyclic side-chains. While the glass transition temperature of P*mmp*F4 is a strong function of R and can be varied between 35 °C and 197 °C for constant backbone structure and molecular weight, solubility cannot be improved by using longer linear or branched side chains. Density functional theory calculations suggest significant polarization-type non-covalent interactions between tetrafluoro-benzene and the biphenol-based monomer as origin for the observed limited solubility, which guide the design of both kinked and straight conjugated polymers with high molar mass and solubility.

Introduction

Polyarylenes offer unique thermal and chemical stability compared to most aliphatic polymers.[1,2] Other aromatic polymers like aromatic polyesters, polyaramides or aromatic polycarbonates contain heteroatom-bonding in their backbone and therefore lack the inherent stability of aryl–aryl bonds. Aromatic carbon bonds are stable against common acids, bases and redox agents that other polymers may suffer from due to their backbones containing functional groups such as esters, carbonates, amides and ethers.[3,4] The presence of aromatic rings in the repeat unit also causes high glass transition temperatures in polyarylenes, as generally observed when cyclic units are incorporated into polymer backbones.[5] High glass transition temperatures are caused by the lower degree of freedom of planar (aromatic) rings in which individual atoms

can only move simultaneously by rotation as a single unit.[6] This low degree of freedom is often accompanied by liquid crystallinity or even fully crystalline properties.[2,5] However, high T_gs and high crystallinity may cause brittleness of materials. This may be mitigated by addition of aliphatic side chains to an aromatic polymer backbone. Thereby solubility improves due to addition of degrees of freedom in the flexible side chain while maintaining a durable polymer backbone. Nonetheless, *para*-polyarylenes are brittle materials due to their low entanglement density caused by their rigidity and rod-like shape.[7,8] However, pioneering work by Schlüter *et al.* on polyarylenes with *meta*-comonomers proved that sufficient entanglement could be generated at very high molecular weights.[7,9,10] These poly(*meta*-/*para*-polyarylenes) (P*mp*P) are tough, amorphous materials on par with aromatic polycarbonates. Yet improved mechanical properties can be achieved by incorporating a "double *meta*-" motif developed by our group.[11] Here the resulting poly(*meta*-/*meta*-/*para*-polyarylenes) (P*mmp*P) are tough materials without prior purification starting from affordable and scalable building blocks.

The typical cross-coupling variant for the transition metal-catalyzed polycondensation of phenylene-based monomers is the Suzuki–Miyaura reaction.[12] Monomers are typically aryl halides coupled with a main group metal coupling partner. Polyarylenes prepared by direct arylation polymerization (DAP) are especially efficient with respect to atom economy com-

[a] Chemnitz University of Technology, Straße der Nationen 62, 09111 Chemnitz, Germany. E-mail: michael.sommer@chemie.tu-chemnitz.de
[b] Institute for Macromolecular Chemistry, University of Freiburg, Stefan-Meier-Str. 31, 79104 Freiburg, Germany
[c] Leibniz Institute of Polymer Research, Hohe Str. 6, 01069 Dresden, Germany
[d] Freiburg Center for Interactive Materials and Bioinspired Technologies (FIT), University of Freiburg, Georges-Koehler-Allee 105, 79110 Freiburg, Germany
†Electronic supplementary information (ESI) available. See DOI: 10.1039/d0py00973c

pared to other cross coupling reactions.[13–16] Aryl halides are coupled directly with C–H activated arylenes without the need for additional functional groups. 1,2,4,5-Tetrafluorobenzene (*p*F4) has been successfully employed in this regard in order to synthesize copolymers of fluorene or carbazole.[17,18] We were interested in kinked, semifluorinated polyarylenes as the envisaged chemistry involving DAP appears highly attractive in terms of improved atom economy, simple monomers and selective regiochemistry. Usage of F4 as the nucleophile in DAP is also expected to lead to less degradation of functional groups during polycondensation such as protio- or oxidative deborylation.[19–23] Regarding properties, backbone fluorination is generally expected to significantly change material properties in terms of chain rigidity, solubility and order, and thus novel property profiles may become accesible.[24–26] We therefore investigated the copolymerization of commercially available F4 with a series of 2,2′-biphenol bromide-based monomers having a double *meta* motif and different side chains developed by our group. The monomer synthesis employed here includes three simple steps only, does not rely on chromatography or distillation and is easily scalable. The molecular and thermal properties of the resulting polymers P*mmp*F4 are investigated. Density functional theory calculations are finally employed to understand and explain the unexpected, rather limited solubility of P*mmp*F4, and these result may guide the design of other polyarylenes or conjugated polymers in general as well.

Results and discussion

Synthesis

We have screened the copolymerization of F4 with differently substituted 2,2′-biphenol monomers with respect to the solvent, concentration and temperature. The catalytic system itself was Pd_2dba_3/P(*o*-anisyl)$_3$/pivalic acid, a system that has emerged as a universal combination for the synthesis of many conjugated polymers *via* DAP.[13] The side chains R used were isopropyl (3*i*), *sec*-butyl (4*s*), cyclopentyl (5*c*), *n*-hexyl (6*n*), *n*-octyl (8*n*), *n*-decyl (10*n*) and 2-ethylhexyl (EH) (Scheme 1). All entries showed gelation or precipitation at moderate molecular weight. This is in stark contrast to P*mmp*P, which is the non-

fluorinated analog that shows excellent solubility for M_w up to ~100 kg mol^{-1}. We prefer to report M_w values here as M_n values are strongly influenced by oligomer content (see size exclusion chromatography (SEC) curves shown as Fig. S1 and S2†).[11] Therefore, molecular weight is indicative of solubility of the copolymer at the temperature of the reaction. Interestingly, longer side chains did not generally improve solubility. The introduction of branched side chains was beneficial to improve solubility in some cases (4*s* *vs.* 5*c* and 3*i*). Interestingly, usage of EH instead of 6*n* or also 8*n* did not improve solubility significantly neither. These observations are in stark contrast to conjugated polymers where side chain branching is key to increase solubility significantly and for many examples to enable processing at all.[27]

Good solvents for P*mmp*F4 are chloroform, dichloromethane and 1,2-dichloroethane, all of which are unsuitable for cross coupling reactions. Chlorobenzene (CB) is a good solvent for P*mmp*F4 but leads to phenyl-endcapping (see Fig. S14†). The best results were achieved for toluene (Tol) as solvent, 100 °C reaction temperature and a monomer concentration of 0.8 M (Table 1). Despite screening for solvents, side chains and temperature, molecular weights were moderate with values up to $M_{w,SEC}$ ~30 kg mol^{-1}, which sometimes could be slightly increased by fractionation (entries 2a and 8). In general, *meta*-substituted polyarylenes show better solubility compared to *para*-substituted ones.[28] To check whether a substantial increase in solubility of P*mmp*F4 could be achieved by backbone modification, F4 was replaced by 1,2,3,5-tetrafluorobenzene (*m*F4) resulting in "all-*meta*" semifluorinated polyarylenes P*mmm*F4 (Table 1, entry 14 and Scheme 2). However, molar masses of P*mmm*F4 were lower compared to the best conditions of P*mmp*F4, hence further optimization was not attempted.

P*mmp*F4 was characterized by ^{1}H and ^{19}F NMR spectroscopy (Fig. 1a and Fig. S10–S16†). Additionally, the ^{13}C NMR spectrum was recorded for the hexyl derivative (entry 2, Fig. 1b). The rather clean ^{1}H NMR spectra without intense end group signals suggest good molecular weights. To shine light on termination reactions, an end group investigation exemplified by entry 13, was carried out. A comparison of the aromatic protons' region, the monomer *mm* (10*n*) containing the Br end group and 2,2′-(hexyloxy)biphenyl as model compound for H end groups reveals dehalogenation[29] as a major cause for functional group degradation (Fig. S17†). An –OCH$_3$ signal at 3.55 ppm, visible in most polymers, indicates anisyl end groups that arise from the covalent attachment of the ligand P(*o*-anisyl)$_3$.[17] The identification of F4-based end groups from the ^{19}F NMR spectra is straightforward. Proven end groups are –C$_6$F$_4$-H and –C$_6$F$_4$-Ph, which result in characteristic low intensity signals in the ^{19}F NMR spectra (Fig. S10b–S16b†). The –C$_6$F$_4$-Ph end group is only observed when CB was used as solvent for polymerization (Fig. S14b†). The herein found end groups are thus typical for cross coupling reactions and DAP, and thus P*mmp*F4 is not an exception in this regard. Quantification of end group intensities with good accuracy is very challenging, and hence not attempted here. In general,
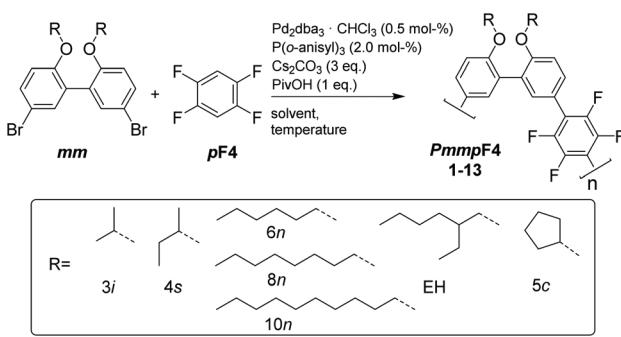

Scheme 1 Synthesis of kinked, semifluorinated P*mmp*F4 *via* DAP.

Table 1 Optimisation of reaction conditions for P*mmp*F4 and P*mmm*F4

Entry #	M1	M2	Solvent	Temp./°C	Conc./M	M_n/kg mol^{-1}	M_w/kg mol^{-1}
1	6*n*	*p*F4	Tol	70	1.0	3.9	8.7
2	6*n*	*p*F4	Tol	100	0.8	10.8	21.5
2a[a]	6*n*	*p*F4	Tol	100	0.8	15.8	31.2
3	6*n*	*p*F4	Tol	120	0.8	3.9	5.5
4	6*n*	*p*F4	THF	100	0.8	7.9	16.8
5	6*n*	*p*F4	Dioxane	100	0.5	6.4	15.0
6	EH	*p*F4	Tol	100	1.2	10.2	14.8
7	4*s*	*p*F4	Tol	100	0.8	10.1	17.1
8[b]	4*s*	*p*F4	Tol	100	0.8	14.4	28.5
9	3i	*p*F4	Tol	100	0.8	1.9	2.5
10	5*c*	*p*F4	Tol	100	0.8	6.6	11.8
11	8*n*	*p*F4	Tol	100	1	6.1	12.6
12	8*n*	*p*F4	CB	90	1	6.2	13.0
13	10*n*	*p*F4	Tol	100	0.8	11.7	20.6
14	6*n*	*m*F4	Tol	100	0.8	8.9	18.8

[a] After Soxhlet extraction with ethyl acetate. [b] A small excess of 0.1 eq. of F4 was used.
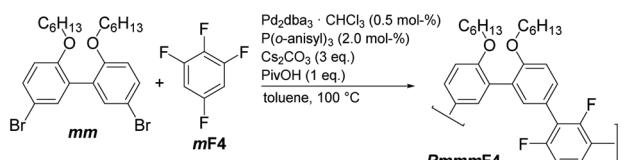
Scheme 2 Synthesis of an all-*meta* semi-fluorinated polyarylene P*mmm*F4.

despite a closer look at typical end groups as well as the use of model compounds, the estimation of absolute molecular weights $M_{n,NMR}$ is not possible for P*mmp*F4. What can be concluded from the synthesis and NMR spectroscopic investigations is that the monomer couple *mm*/F4 is a simple comonomer system that undergoes clean chemistry with typical side/termination reactions. Entries that reached $M_{w,SEC}$ ~20–30 kg mol^{-1} precipitated or gelated independent of the side chain, a property that apparently is inherent to P*mmp*F4.

Thermal properties

The thermal properties were investigated next (Fig. 2). Fig. 2a shows the dependence of T_g of P*mmp*F4 with *n*-hexyl side chains on molecular weight. A trend showing saturation at 90 °C for M_n/M_w ~10/20 kg mol^{-1} is seen, which is expected for conjugated polymers (Table 2).[30] The dependence of the T_g of P*mmp*F4 on the side chain for similar molecular weight is shown in Fig. 2b and Table 2. Usually, longer side-chains decrease the T_g of conjugated polymers.[30–33] This is also seen here, with the T_g of P*mmp*F4 with 10*n* being lower (35 °C) than of P*mmp*F4 with 6*n* (83 °C), as expected.[33] P*mmp*F4 with 4*s* and EH side chains exhibits higher T_gs (173 and 68 °C, respectively) compared to 6*n* and 8*n* (83 and 50 °C, respectively, Fig. 2a, Table 2). The increase from T_g for linear to branched side chains at a constant number of carbons in the side chain is again similar to *e.g.* polythiophenes, where for poly(3-octylthiophene) and poly(3-(2-ethylhexyl)thiophene) glass transition temperatures of −13 °C and 24 °C, respectively, have been reported.[31,34] The T_g of P*mmp*F4 further increases more strongly when moving to cyclic side chains. Upon attaching 5*c* side chains a T_g of 197 °C is measured. Clearly, cyclic side chains increase T_g much stronger than linear ones. While cyclic side chains are rather uncommon for conjugated polymers, the comparison of the T_gs of poly(1-hexene) (−63 °C)[35] and polyvinylcyclohexane (80 °C)[36] also indicates a strong increase in T_g for linear *versus* cyclic side chains at constant side chain fraction. We also attempted to install cyclohexyl
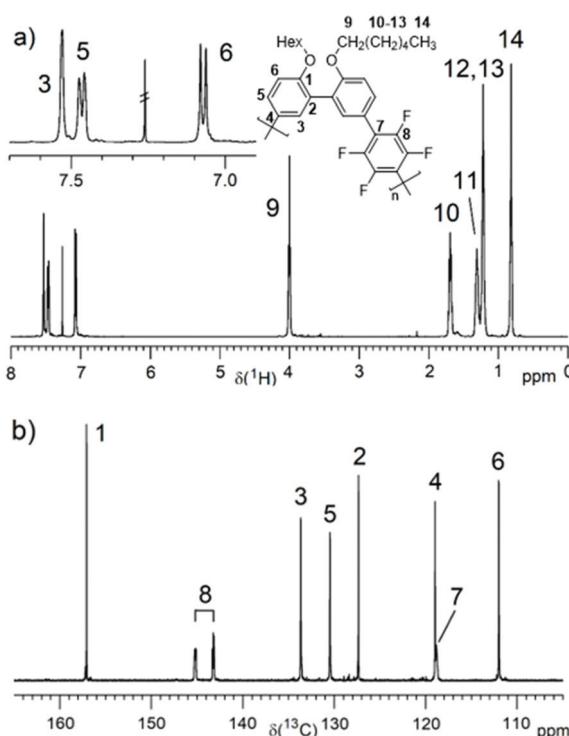
Fig. 1 ^{1}H (a) and ^{13}C (b) NMR spectra of P*mmp*F4 (entry 2) in CDCl$_3$ with assignments.
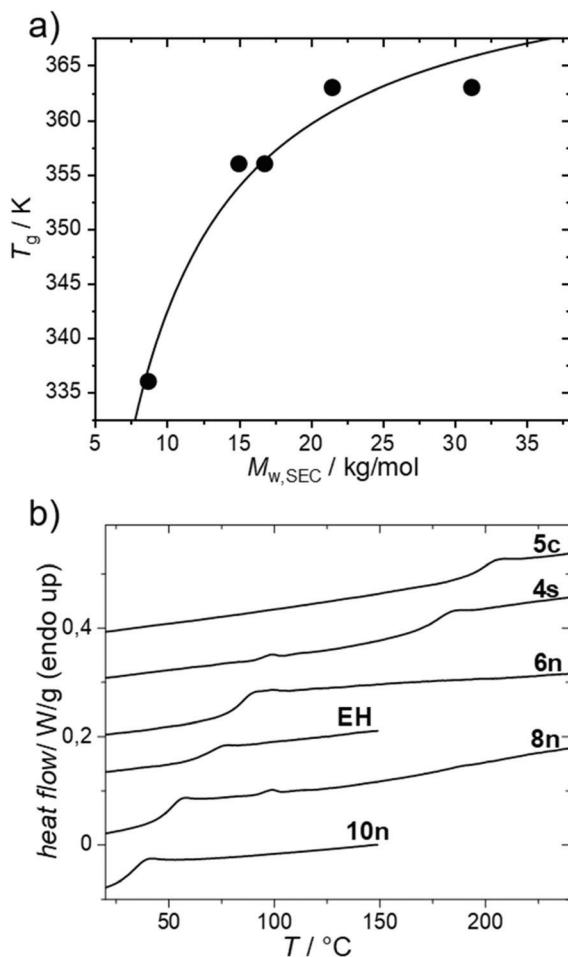
Fig. 2 Glass transition temperature of P*mmp*F4 from differential scanning calorimetry with **6n** as a function of molecular weight (a) and for varying side chains including entry 5 (b). Conditions: 2nd heating, 10 K min^{−1}, N$_2$.

Table 2 Glass transition temperatures of polyarylenes with different side chains

Entry #	R=	T_g/°C	M_w/kg mol^{-1}	Đ
2a	*n*-Hexyl	90	31.2	1.5
2	*n*-Hexyl	90	21.5	2.0
4	*n*-Hexyl	83	16.8	2.1
5	*n*-Hexyl	83	15.0	2.3
1	*n*-Hexyl	63	8.7	2.2
7	*s*-Butyl	173	17.1	1.7
10	Cyclopentyl	197	11.8	1.8
12	*n*-Octyl	50	13.0	2.1
6	(2-Ethyl) hexyl	68	14.8	1.5
13	*n*-Decyl	35	20.6	1.8

side chains, which failed at the monomer synthesis stage where mono-substituted products were obtained (not shown). Thus, the T_g of P*mmp*F4 can be varied by as much as ~160 K for the herein investigated range of side chains.

With P*mmp*P being highly soluble,[11] it is tempting to explain the limited solubility of P*mmp*F4 by the replacement of

Ph by F4. However, the mere presence of an F4 moiety in the backbone alone cannot explain the limited solubility. Other alternating F4 copolymers with fluorene (PF8F4) or carbazole show excellent solubility with molecular weights of PF8F4 of up to $M_{n,SEC}$ = 347 kg mol^{-1}.[17] With PF8F4 exhibiting stiff and coplanar dioctylfluorene units in combination with *p*F4, it appears counterintuitive that the herein investigated twisted and kinked P*mmp*F4 with a similar amount of side chains exhibits a lower solubility than PF8F4 for the same range of solvents. We therefore assumed attractive interactions between segments of P*mmp*F4 to be present. Possible interactions anticipated include oxygen/lone pair-F4 interactions, which may be comparable to anion/lone pair-π-interactions, and π–π interactions (Fig. 3a and b).[37,38]

However, F4-oxygen interactions as depicted in Fig. 3a are difficult to prove. The fact that the solubility of P*mmp*F4 in THF was even lower than in Tol did also not point to such a motif. Interactions including π–π-stacked configurations as depicted in Fig. 3b were therefore investigated theoretically.

DFT calculations

In order to further investigate a possible origin for the reduced solubility of P*mmp*F4, we have performed an extensive theoretical study of the weak interactions between its building blocks. The absence of effects due to the side chains suggests that strong interactions between different parts of the P*mmp*F4 backbone might be responsible for the decreased solubility relative to P*mmp*P observed. We were particularly interested in the effect of fluorination of the phenyl-based comonomer and the role of substitution of the biphenyl comonomer on the aggregation behavior. We therefore studied the interaction of building blocks of P*mmp*F4 as well as differently substituted derivatives. Fig. 3c shows chemical structures of all compounds involved, namely C_6H_6, $C_6H_2F_4$, C_6F_6, $C_{15}H_{14}$, $C_{16}H_{18}$ and $C_{14}H_{14}O_2$.

The density functional theory (DFT) calculations were performed in the projector augmented wave method[39] as implemented in the GPAW package.[40,41] The smooth Kohn–Sham wave functions were represented on real space grids
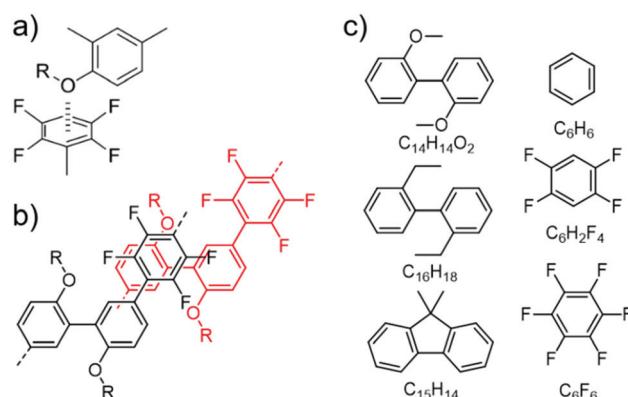

Fig. 3 (a and b) Possible chain chain interactions of P*mmp*F4 and (c) model compounds used for DFT calculations.

with a grid spacing of 0.2 Å and the electron density on grids of 0.1 Å spacing. The exchange–correlation energy was approximated as devised by Perdew, Burke and Ernzerhof (PBE)[42] and the corrections proposed by Tkatchenko and Scheffler (TS09)[43] were included to describe dispersive interactions. The results were cross checked using the vdW-DF2 [44] functional. The structures were set up using the atomic simulation environment[41] and the simulation box was ensured to contain at least 4 Å of space around each atom. Molecules were placed in random relative orientations and structures subsequently relaxed to the next local minimum. This resulted in 190–650 relaxed structures for each pairing from which we have obtained the configurations of lowest energy. The configurations were accepted if at least two lowest energy structures were found within the range of 4 kJ mol^{-1} representing chemical accuracy (see Fig. S19†).[45] Interactions involving $C_6H_2F_4$ required considerably more pairs than those containing C_6H_6 or C_6F_6 to achieve this goal. This effect can be attributed to the lower symmetry of $C_6H_2F_4$, which results in a larger structural entropy in the pairs.

Fig. 4a displays the binding energies (BEs, positive values indicate attraction) of the energetically best pairs found. There is a clear trend of enhanced attraction between fluorinated species as compared to benzene. The lowest BE is found for the benzene pair with 15 kJ mol^{-1} in the parallel-displaced configuration (see Fig. S20†). This value is slightly higher than the CCSD(T) value of 11–12 kJ mol^{-1} (ref. 46 and 47) and the

difference can be assigned to the tendency of the TS09 approximation to overestimate the interactions,[48] while keeping the relative ordering correct.[49] We find the C_6H_6–C_6F_6 pair to bind with 42 kJ mol^{-1} in good agreement to MP2 value of 39 kJ mol^{-1}.[50] The overall highest BE between benzene and its fluorinated versions is found for the C_6F_6 pair with 52 kJ mol^{-1}. All combinations involving C_6H_6, $C_6H_2F_4$ and C_6F_6 prefer parallel-displaced configurations.

Regarding relaxed structures between C_6H_6, $C_6H_2F_4$ and C_6F_6 with $C_{15}H_{14}$, $C_{16}H_{18}$ and $C_{14}H_{14}O_2$, there is a large variety of relative configurations with the tendency to parallel stacked configurations of the fluorinated benzenes with the biphenyl model compounds (see Fig. 3b, 4b and S16†). Also here, the BEs follow clear trends of stronger interactions with increasing number of fluorine substituents for each biphenyl derivative. Pairs involving $C_{14}H_{14}O_2$ in combination with C_6H_6 and $C_6H_2F_4$ are found to form CH-O hydrogen bonds (see Fig. S20†) with bond lengths between 2.7 Å and 2.9 Å for the two best structures of each pair, which obviously are not relevant for the polymer under scrutiny. However, from a general perspective, this structure factor is remarkable despite of the weakness of this bond that should be less than 10 kJ mol^{-1}.[51,52] Most importantly, however, is the finding that all three benzene derivatives exhibit the strongest interactions with $C_{14}H_{14}O_2$. A higher BE is found for $C_{14}H_{14}O_2$ and C_6H_6, $C_6H_2F_4$ as well as C_6F_6 in comparison to the coplanar fluorene derivative $C_{15}H_{14}$. $C_{16}H_{18}$ shows nearly identical BEs indicating the presence of oxygen to be the decisive factor for enhanced interaction. A cross check with the conceptually different description of dispersive interactions by the vdW-DF2 functional leads to slightly lower binding energies, but retains the same relative ordering as seen in Fig. 4c. A similar behaviour is already obtained at the PBE level (evaluated for TS09 relaxed structures), which indicates that the effect is rather due to polarization than dispersion.[53] Bader analysis[54,55] did not reveal any significant charge transfer in these structures.

The larger BE values of the couple $C_{14}H_{14}O_2$/C_6F_6 compared to $C_{15}H_{14}$/C_6F_6 reflect both the rather good solubility of PF8F4 [17] as well as the limited solubility of P*mmp*F4. Furthermore, these polar backbone interactions help to understand the rather small influence of side chain length on solubility, which is uncommon for aromatic polymers. From a structural design point of view, the combination of the F4 motif with alkoxylated biphenyls apparently makes a large difference, as the increase of chain–chain interactions leads to reduced solubility. A further interesting observation is that the clear trends in BEs as shown in Fig. 4 are only found when a *trans*-conformation of the biphenyl model structure of $C_{14}H_{14}O_2$ (Fig. 3c) is used as starting point. Starting from the corresponding *cis*-conformation also yields somewhat larger BE values for the fluorinated phenyls, but the trends are less clear and the relative differences in BE values lower (Fig. 5).

The *cis*/*trans* effect is nearly vanishing for $C_{16}H_{18}$. This may indicate that such *trans*-conformations are present in the copolymer and present an important contribution to the observed solubility behaviour. Restricting the presence of *trans*-confor-
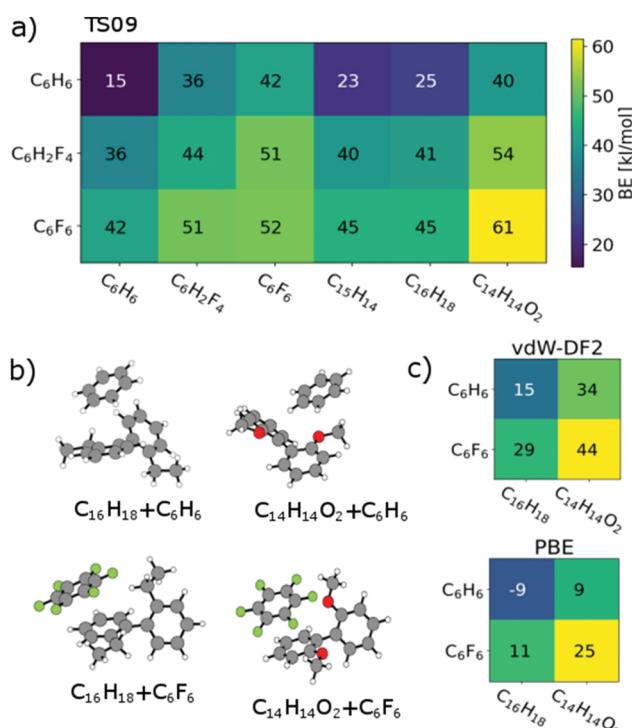
Fig. 4 (a) Scheme of binding energies between the model fragments of P*mmp*F4, for chemical structures see Fig. 3c. (b) Selected lowest energy structures. (c) Binding energies in vdW-DF2 and PBE in the TS09 relaxed structure.
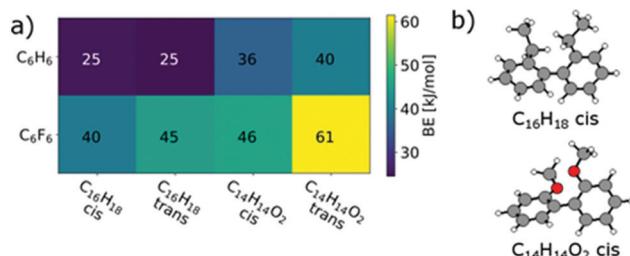
Fig. 5 (a) *cis/trans* effect in C$_{16}$H$_{18}$ and in C$_{14}$H$_{14}$O$_2$ on the binding energies to C$_6$H$_6$ and C$_6$F$_6$. (b) *cis* configurations of C$_{16}$H$_{18}$ and C$_{14}$H$_{14}$O$_2$.

mations by conformational locking may therefore address the limited solubility of P*mmp*F4.

Conclusions

We have successfully prepared semifluorinated, kinked polyarylenes P*mmp*F4 by a straightforward and simple direct arylation approach with high atom economy. The glass transition temperature of these semifluorinated aromatic copolymers can be varied between 35 and 197 °C depending on type and size of the side chain. Molar mass is limited by solubility and not by termination reactions, which is surprising considering the kinked backbone structure and the exceptionally good solubility of the non-fluorinated analog P*mmp*P. Density functional theory calculations on model systems reveal strong attractive interactions between the fluorinated and dialkoxylated comonomers, which continuously increase with the degree of fluorination. This effect is caused mainly by an increased polarization interaction rather than changes in dispersion or charge transfer. It is thus the combination of the alkoxy side chains with the F4 unit that causes the experimentally observed limited solubility, which should be avoided if copolymers with high molar mass and solubility are the target.

Conflicts of interest

There are no conflicts to declare.

Acknowledgements

Notes and references

1 E. J. Park and Y. S. Kim, *J. Mater. Chem. A*, 2018, **6**, 15456–15477.

2 M. Friedman and G. Walsh, *Polym. Eng. Sci.*, 2002, **42**, 1756–1788.

3 A. D. Mohanty, S. E. Tignor, J. A. Krause, Y.-K. Choe and C. Bae, *Macromolecules*, 2016, **49**, 3361–3372.

4 S. Noh, J. Y. Jeon, S. Adhikari, Y. S. Kim and C. Bae, *Acc. Chem. Res.*, 2019, **52**, 2745–2755.

5 J. A. Reglero Ruiz, M. Trigo-López, F. C. García and J. M. García, *Polymers*, 2017, **9**, 414.

6 I. A. Ronova and S. S. A. Pavlova, *High Perform. Polym.*, 1998, **10**, 309–329.

7 R. Kandre, K. Feldman, H. E. H. Meijer, P. Smith and A. D. Schlüter, *Angew. Chem., Int. Ed.*, 2007, **46**, 4956–4959.

8 S. Jakob, A. Moreno, X. Zhang, L. Bertschi, P. Smith, A. D. Schlüter and J. Sakamoto, *Macromolecules*, 2010, **43**, 7916–7918.

9 R. Kandre and A. D. Schlüter, *Macromol. Rapid Commun.*, 2008, **29**, 1661–1665.

10 B. Hohl, L. Bertschi, X. Zhang, A. D. Schlüter and J. Sakamoto, *Macromolecules*, 2012, **45**, 5418–5426.

11 F. Kempe, O. Brügner, H. Buchheit, S. N. Momm, F. Riehle, S. Hameury, M. Walter and M. Sommer, *Angew. Chem., Int. Ed.*, 2018, **57**, 997–1000.

12 J. Sakamoto, M. Rehahn, G. Wegner and A. D. Schlüter, *Macromol. Rapid Commun.*, 2009, **30**, 653–687.

13 M. Wakioka and F. Ozawa, *Asian J. Org. Chem.*, 2018, **7**, 1206–1216.

14 J.-R. Pouliot, F. Grenier, J. T. Blaskovits, S. Beaupré and M. Leclerc, *Chem. Rev.*, 2016, **116**, 14225–14274.

15 J. Kuwabara and T. Kanbara, *Bull. Chem. Soc. Jpn.*, 2018, **92**, 152–161.

16 R. M. Pankow and B. C. Thompson, *Polym. Chem.*, 2020, **11**, 630–640.

17 M. Wakioka, Y. Kitano and F. Ozawa, *Macromolecules*, 2013, **46**, 370–374.

18 W. Lu, J. Kuwabara and T. Kanbara, *Macromolecules*, 2011, **44**, 1252–1255.

19 A. D. Schlüter and J. P. Rabe, *Angew. Chem., Int. Ed.*, 2000, **39**, 864–883.

20 M. Sommer, H. Komber, S. Huettner, R. Mulherin, P. Kohn, N. C. Greenham and W. T. S. Huck, *Macromolecules*, 2012, **45**, 4142–4151.

21 S. Kappaun, M. Zelzer, K. Bartl, R. Saf, F. Stelzer and C. Slugovc, *J. Polym. Sci., Part A: Polym. Chem.*, 2006, **44**, 2130–2138.

22 T. Kirschbaum, R. Azumi, E. Mena-Osteritz and P. Bäuerle, *New J. Chem.*, 1999, **23**, 241–250.

23 M. Jayakannan, J. L. J. van Dongen and R. A. J. Janssen, *Macromolecules*, 2001, **34**, 5386–5393.

24 K. D. Deshmukh, R. Matsidik, S. K. K. Prasad, N. Chandrasekaran, A. Welford, L. A. Connal, A. C. Y. Liu, E. Gann, L. Thomsen, D. Kabra, J. M. Hodgkiss, M. Sommer and C. R. McNeill, *ACS Appl. Mater. Interfaces*, 2018, **10**, 955–969.

25 X. Liao, F. Wu, Y. An, Q. Xie, L. Chen and Y. Chen, *Macromol. Rapid Commun.*, 2017, **38**, 1600556.

26 A. Nitti, F. Debattista, L. Abbondanza, G. Bianchi, R. Po and D. Pasini, *J. Polym. Sci., Part A: Polym. Chem.*, 2017, **55**, 1601–1610.

27 M. L. Tang and Z. Bao, *Chem. Mater.*, 2011, **23**, 446–455.

28 R. Pinal, *Org. Biomol. Chem.*, 2004, **2**, 2692–2699.

29 F. Lombeck, R. Matsidik, H. Komber and M. Sommer, *Macromol. Rapid Commun.*, 2015, **36**, 231–237.

30 C. Müller, *Chem. Mater.*, 2015, **27**, 2740–2754.

31 S. Pankaj, E. Hempel and M. Beiner, *Macromolecules*, 2009, **42**, 716–724.

32 Z. Qian, Z. Cao, L. Galuska, S. Zhang, J. Xu and X. Gu, *Macromol. Chem. Phys.*, 2019, **220**, 1900062.

33 R. Xie, A. R. Weisen, Y. Lee, M. A. Aplan, A. M. Fenton, A. E. Masucci, F. Kempe, M. Sommer, C. W. Pester, R. H. Colby and E. D. Gomez, *Nat. Commun.*, 2020, **11**, 1–8.

34 L. Yu, E. Davidson, A. Sharma, M. R. Andersson, R. Segalman and C. Müller, *Chem. Mater.*, 2017, **29**, 5654–5662.

35 M. H. Jandaghian, A. Soleimannezhad, S. Ahmadjo, S. M. M. Mortazavi and M. Ahmadi, *Ind. Eng. Chem. Res.*, 2018, **57**, 4807–4814.

36 J. S. Grebowicz, *Polym. Eng. Sci.*, 1992, **32**, 1228–1235.

37 N. J. Singh, H. M. Lee, I.-C. Hwang and K. S. Kim, *Supramol. Chem.*, 2007, **19**, 321–332.

38 S. Kozuch, *Phys. Chem. Chem. Phys.*, 2016, **18**, 30366–30369.

39 P. E. Blöchl, *Phys. Rev. B: Condens. Matter Mater. Phys.*, 1994, **50**, 17953–17979.

40 J. J. Mortensen, L. B. Hansen and K. W. Jacobsen, *Phys. Rev. B: Condens. Matter Mater. Phys.*, 2005, **71**, 035109.

41 J. Enkovaara, C. Rostgaard, J. J. Mortensen, J. Chen, M. Dulak, L. Ferrighi, J. Gavnholt, C. Glinsvad, V. Haikola, H. A. Hansen, H. H. Kristoffersen, M. Kuisma, A. H. Larsen, L. Lehtovaara, M. Ljungberg, O. Lopez-Acevedo, P. G. Moses, J. Ojanen, T. Olsen, V. Petzold, N. A. Romero, J. Stausholm-Møller, M. Strange, G. A. Tritsaris, M. Vanin, M. Walter, B. Hammer, H. Häkkinen, G. K. H. Madsen, R. M. Nieminen, J. K. Nørskov, M. Puska, T. T. Rantala, J. Schiøtz, K. S. Thygesen and K. W. Jacobsen, *J. Phys.: Condens. Matter*, 2010, **22**, 253202.

42 J. P. Perdew, K. Burke and M. Ernzerhof, *Phys. Rev. Lett.*, 1996, **77**, 3865–3868.

43 A. Tkatchenko and M. Scheffler, *Phys. Rev. Lett.*, 2009, **102**, 073005.

44 K. Lee, É. D. Murray, L. Kong, B. I. Lundqvist and D. C. Langreth, *Phys. Rev. B: Condens. Matter Mater. Phys.*, 2010, **82**, 081101.

45 J. A. Pople, *Rev. Mod. Phys.*, 1999, **71**, 1267–1274.

46 Y. C. Park and J. S. Lee, *J. Phys. Chem. A*, 2006, **110**, 5091–5095.

47 E. Miliordos, E. Aprà and S. S. Xantheas, *J. Phys. Chem. A*, 2014, **118**, 7568–7578.

48 A. Tkatchenko, R. A. DiStasio, R. Car and M. Scheffler, *Phys. Rev. Lett.*, 2012, **108**, 236402.

49 M. Hassan, M. Walter and M. Moseler, *Phys. Chem. Chem. Phys.*, 2013, **16**, 33–37.

50 S. Tsuzuki, T. Uchimaru and M. Mikami, *J. Phys. Chem. A*, 2006, **110**, 2027–2033.

51 S. Scheiner, T. Kar and J. Pattanayak, *J. Am. Chem. Soc.*, 2002, **124**, 13257–13264.

52 D. Ž. Veljković, G. V. Janjić and S. D. Zarić, *CrystEngComm*, 2011, **13**, 5005–5010.

53 J. Badorrek, M. Walter and M.-P. Laborie, *J. Renewable Mater.*, 2018, **6**, 325–335.

54 R. F. W. Bader, *Atoms in Molecules: A Quantum Theory*, Clarendon Press, Oxford England: New York, 1st Paperback edn, 1994.

55 W. Tang, E. Sanville and G. Henkelman, *J. Phys.: Condens. Matter*, 2009, **21**, 084204.